ELECTROMAGNETIC WAVE SCATTERING EXPERIMENTS IN HALL THRUSTER PLASMA PLUMES

Brian E. Gilchrist‡, Christopher N. Davis*, Douglas O. Carlson*, Shawn G. Ohler, and Alec D. Gallimore§
University of Michigan
Ann Arbor, MI

Abstract

The interactions of an electromagnetic (EM) wave propagating through plasma plumes of modern electric propulsion systems include both phase change and attenuation. Significant effects can exist even if the EM wave frequency is well above the local plasma frequency of the plume. Experimental measurements of spectral characteristics and theoretical analyses have shown that temporal responses modulate the EM wave by both amplitude and phase modulation. This paper will discuss the spectrums measured for Hall Thrusters (SPT-100, D-55, and UM P-5). The paper compares the measured spectrums of these thrusters to a calculated spectrum using ray tracing based on an axial and azimuthal model of density oscillation. It will be shown that an azimuthal model provides a better match to measured data, though more work needs to be done to experimentally show the existence of an azimuthal perturbation within the plume of a Hall thruster.

Nomenclature

E	Electric field (V/m)
k	Wave number (m^{-1})
m_{amp}, m_{freq}, m_{phase}	Modulation Factors for amplitude (unitless), frequency (rad/s), phase (rad), and density noise or oscillations (unitless)
n_e	Electron number density (cm^{-3})
n_C	Critical electron density (cm^{-3})
$n_{e(x,y,t)}$	Electron density as a function of time and space at a fixed axial position (cm^{-3})
$n_{e(x,y)}$	Electron density as a function of space at a fixed axial position (cm^{-3})
r	Radial distance from thruster.
z	Axial distance from thruster
s	Position of ray
t	Time (s)
ϕ_{vacuum}	Phase shift due to free space
ϕ_{plasma}	Phase shift due to plasma
$\Delta\phi$	Phase shift of propagated wave relative to phase with out a plasma
$\phi(t)$	Phase of wave at time, t (rad)
λ	Wavelength (m)
σ	Standard deviation (width) of azimuthal instability (cm)
ω	Radial frequency (rad/sec)
ω_m	Modulation frequency (rad)
J_n	Nth order Bessel function
ω_o	carrier frequency (rad)
m	Instability height (unitless)
d	Distance from center of plasma to instability (cm)

Introduction

Recently, there have been results reported on the use of microwave interferometers as highly accurate, non-intrusive diagnostic tools in the plumes of Hall and arcjet electric propulsion thrusters [1, 2]. Other studies have measured and modeled the impact of microwave signal propagation through these plasma plumes to assess their impact on spacecraft communication, radar, or radio navigation systems [2, 3, 9]. In general, it has been shown that for present day, kilowatt-class Hall thrusters, significant attenuation is primarily observed in the lower microwave frequency bands (below about 8 GHz) principally due to refractive spreading effects [1, 2]. However, phase modification of electromagnetic wave (EM) signals is significant throughout the microwave frequency range to above 20 GHz and well out in the plume [2]. Further, both amplitude and phase temporal variations can generate frequency sidebands on microwave EM signals propagating through plumes such as seen in Figure 1 for an SPT-100 Hall thruster [2, 3]. These effects will become even more significant as power levels for Hall thrusters increase.

In this paper we will first discuss the general theory of EM waves propagating through a plasma and how ray tracing was used to model the effect. We will also briefly review the types of oscillation present in Hall thrusters. Finally, we will discuss the axial and azimuthal temporal models as a method of modeling the time variation or oscillations of the plasma plume of a Hall Thruster and then compare the calculated spectrum from these models for the SPT-100, D-55, and UM Thruster to measured spectrums.

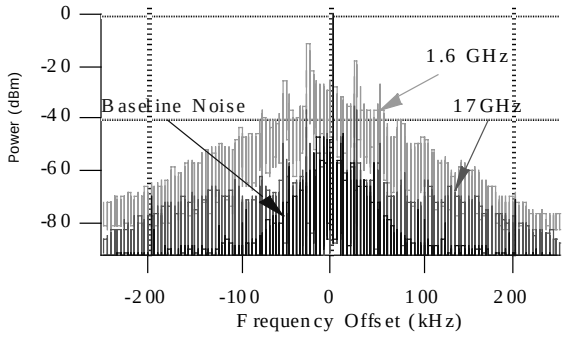

Figure 1 – Spectral response of the SPT-100 at 1.6 and 17 GHz [3].

Theoretical Background

This section will begin with a review of amplitude and phase modulation of an electromagnetic wave. Then it will go on to discuss the theory of ray tracing which was used to keep track of the phase and amplitude changes as a function of time of a wave propagating through a plasma, and finally the section will give a brief overview of the types of instabilities present in Hall thrusters.

Electromagnetic Wave Interactions

A plane wave propagating through a plasma can be modulated both in phase and in amplitude. The following is a mathematical summary of amplitude and phase modulation

Suppose we have a plane wave

$$E(r) = E_o(\bar{r})\cos(w_o t) \tag{1}$$

Pure amplitude modulation is represented as

$$E(\bar{r}) = E_o(\bar{r})\cos(w_o t)(1 + m_{amp}\cos(w_m t)) \tag{2}$$

which can be expanded via a well known trigonometric identity to

$$E(\bar{r}) = E_o(\cos(w_o t) + \frac{m_{amp}}{2}\left[\cos((w_o + w_m)t) + \cos((w_o - w_m)t)\right] \tag{3}$$

Here m_{amp} is a modulation fraction and ω_m is the modulation frequency. In the above expression we see explicitly contributions from the original signal plus the first sidebands.

Similarly, using phasor notation, pure phase modulation may be represented by

$$E(\bar{r}) = E_o(\bar{r})\exp(j(w_o t + m_{phase}\cos(w_p t))) \tag{4}$$

Here m_{phase} is a modulation fraction and ω_p is the modulation frequency. Recall when using phasor notation, to obtain physical field we must take the real part of $E(r)$. The frequency spectrum may be obtained by expanding the exponential in terms of Bessel functions of the first kind. We use the following identity,

$$\exp(jx\cos(\theta)) = \sum_{n=-\infty}^{\infty} j^n J_n(x)\cos(n\theta) \tag{5}$$

where $J_n(x)$ is the n-th Bessel function. Expanding and taking the real part yields

$$\begin{aligned} E(\bar{r}) = E_o(\bar{r})(&J_o(m_{phase})\cos(w_o t) \\ &- J_1(m_{phase})(\sin(w_o + w_p)t + \sin(w_o - w_p)t) \\ &+ J_2(m_{phase})(\cos(w_o + 2w_p)t - \cos(w_o - 2w_p)t) \\ &+ \ldots) \end{aligned} \tag{6}$$

Whereas pure amplitude modulation gives rise only to the first harmonics, pure phase modulation gives rise to an infinitude of harmonics. If the argument m_{phase} is less than one, the magnitude of the Bessel function decrease as the frequency of the harmonics increase.

Ray Tracing of EM Waves

Ray tracing separates the components of the electromagnetic fields so that the amplitude, phase, and path are traced individually. The attenuation and phase of the signal are predicted by integrating the wave number along the ray path. The attenuation is predicted through the imaginary part of the wave number which is negligible in the thrusters studied [4], and the phase is tracked (7c) by using the real part of the wave number (7a)

$$k(\bar{r},t) = \frac{\omega}{c}\sqrt{1 - \frac{\omega_p^2(\bar{r},t)}{\omega^2}} = \omega\sqrt{\mu_o \varepsilon_o \varepsilon_r(\bar{r},t)} \tag{7a}$$

$$\omega_p^2(\bar{r},t) = \frac{n_e(\bar{r},t)e^2}{\varepsilon_o m_e} \tag{7b}$$

$$\phi_2(s_2) - \phi_1(s_1) = \int_{s_1}^{s_2} k(\bar{r},t)\,ds \tag{7c}$$

The ray path then follows the gradients of electron density

$$\frac{\partial}{\partial s}\left[\sqrt{\varepsilon_r(\bar{r},t)}\hat{s}\right]=\nabla\sqrt{\varepsilon_r(\bar{r},t)} \quad (8)$$

where the relative permittivity is related to the electron number density through Equations 7a and 7b

Using these basic equations and a temporal and spatial density model (to be described later), the spectrum for a wave transversing the plume of a hall thruster can be predicted. The ray tracing analysis is applied to transmission paths in a plane orthogonal to the flow of plasma. The basic geometry is shown below in figure 2.

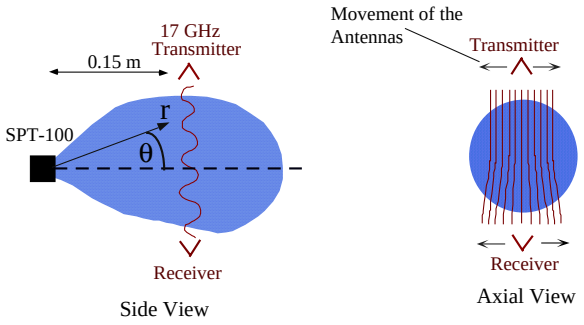

Figure 2 – Physical system for ray trace modeling.

Hall Thruster Instability Summary

Here we briefly summarize the kinds of oscillations that occur inside the SPT acceleration channel. A more detailed review has been given by Choueiri [5]. As the ions and their associated electrons are accelerated into the plume, time variation in the local electron density in the plume may be affected. The oscillations include low frequency azimuthal drift waves, axially propagating "transit-time" oscillations, high frequency azimuth drift waves, ionization instability waves and wave emission associated with weakly ionized, inhomogeneous plasma in crossed electric and magnetic fields.

In addition to Hall thruster type, operating conditions of the thruster also affect the frequency range characteristic of different instabilities. For the instabilities below, the general operating conditions are as follows [5]: diameter of acceleration channel (~10cm), discharge voltage (U_d=200V), mass flow rate (dm/dt = 3 g/s of Xe), and, discharge current (I_d = 3-3.2 A).

Oscillations between 1 and 20 kHz are sensitive to the circuitry of the thruster and are relatively non existent under nominal operating conditions. Between 20 and 60 kHz a type of low frequency azimuthal propagating wave is present [5,6]. These are excited predominantly near the exit plane of the thruster in the vicinity of negative gradient of the mostly radial magnetic field (dBr/dz < 0, where dz is along the axial direction). The strength of these waves is dependent on the operation region (I-V curve). For instance, these waves are dominant at low discharge voltage U_d and diminish in the current saturation region.

Between 20 and 100 kHz exist axially propagating waves which are bounded by the ion collision frequency (~20 kHz) and the electron collision frequency (~200 kHz). Contained in this region is the ionization frequency (~35 kHz). Oscillations between 70 and 500 kHz also known as "transit-time" oscillations are turbulent [7]. The frequency is related to ion velocity v_0 and the length of the acceleration channel L, by $f = v_0/L$. Finally there exist a host of high frequency oscillations where f > 0.5 MHz. These tend to dominate during nominal operation of the thruster. One type of high frequency oscillation is mostly azimuthal and was the first to be predicted theoretically [8]. Besides this type, other high frequency oscillations have not been well studied.

Axial Model of Electron Density

In the axial model, the electron density is assumed to vary as a function of time according to the following equation [9].

$$n_{temp}(t)=1+m\cos(k\bullet r-\omega t) \quad (9)$$

The total electron density as a function of space and time can then be written as

$$n(r,t)=n(r)\times(1+m\cos(k\bullet r-\omega t)) \quad (10)$$

where n(r) is the static electron density profile of an SPT-100 given in [3]. For the SPT-100, the parameters of the time varying density were found to be the following [9]

m=.12, ω=2π*26e3 rad/s, k = 10.9

Simulations Using Axial Model

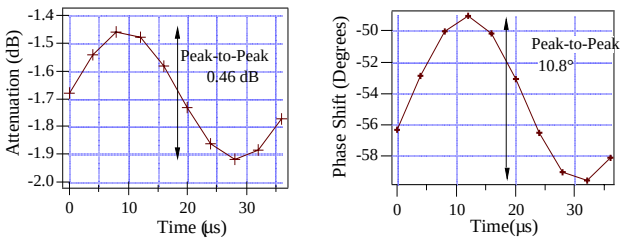

Figure 3 – Simulated amplitude and phase variations for axial model

Figure 3 shows the simulated amplitude and phase over time using the axial model for a 17 GHz signal transmitted through the plume .15 m from the exit plane of an SPT-100 model thruster. See [2] for more details on the calculations. The amplitude and phase values shown are relative to the power or phase shift present with no plume.

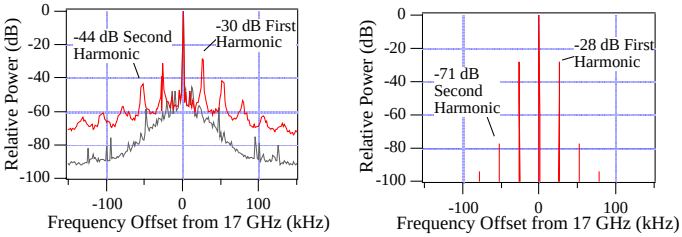

Figure 4– Comparison of the measured and simulated power spectral density of a 17 GHz signal transmitted across the plume .15 m from the exit plane.

As can be seen from figure 4, the axial model does not correctly predict the second or higher order harmonics suggesting that the model is not completely accurate.

Azimuthal Model

In the rotational model, the electron density as a function space and time was based on an azimuthal instability as opposed to an axial in the thruster's plume. The instability was superimposed on the thruster's static (time-averaged) electron density profile. It was assumed that the azimuthal instability rotated around the center of the plume at a certain constant angular velocity, ω. Figure 5 shows a three dimensional representation of the plasma and the instability. This is just a illustrative diagram and is not an actual snap shot of the plume. We modeled the instability as a Gaussian distribution with a width, σ, height, m, and distance from the center of the plume, d, as shown in Figure 6. The total electron density (without rotation taken into account) can then be shown mathematically as

$$n(x,y) = n(x,y) \times (1 + me^{-\sigma((x-d)^2+(y-d)^2)}) \qquad (11)$$

where n(x,y) is the static electron distribution at a given axial position and is symmetric about the origin of the plasma plume. For the purposes of our model, we assume the static electron density also has a Gaussian distribution with a σ equal to 7.5 cm and a peak density of 10^{11} cm^{-3}.

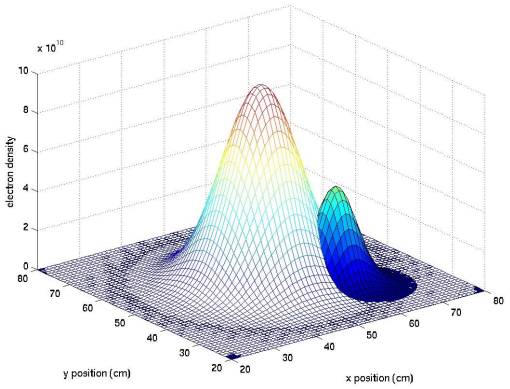

Figure 5 – 3-dimensional view of static electron density and the azimuthal instability

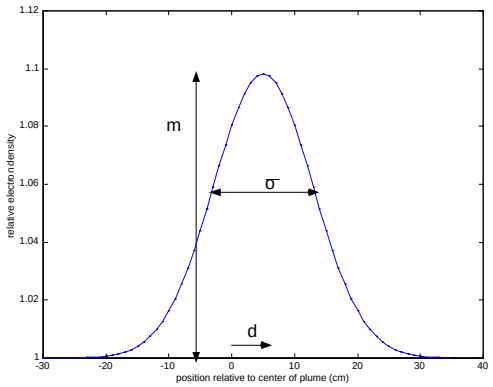

Figure 6 – 2-dimensional representation of the azimuthal instability model where m is the relative amplitude of the instability with respect to the total electron density, σ is the width, and d is the distance the instability is from the origin.

Comparison with Measurements

The two sets of figures below show the comparison of the spectrum generated by using the rotational model and ray tracing techniques to that of the measured spectrum. In the D-55 thruster two different spectrums were observed depending of the axial positions while in the UM thruster only one spectrum was observed. All calculations were done slightly off-center of the plasma plume due to the fact that calculations near the center caused double harmonics to appear. See [10] for more details on the spectral measurements of the D-55 and UM thruster.

It was found that an oscillation with a rotational frequency of 100 kHz, height (m) of .06, distance

from the center (d) of 3 cm, and a σ of 4.1 cm gave sidebands very close in amplitude to those observed in the measured spectrum at 10 inches from the exit plane of the D-55 thruster. The simulation results are compared with measurements in Figure 7a and b.

We also generated a simulated spectrum with sideband amplitudes close to those measured in the near field, 4.75 inches, of the D-55 by changing the parameters of the instability as shown in Figure 8a and b. By setting the rotational frequency of the azimuthal oscillation to 100 kHz, its height (m) to .1, the distance from the origin to 3 cm, and σ to 10 cm it was possible to simulate sidebands very close in amplitude to those observed in the measured spectrum.

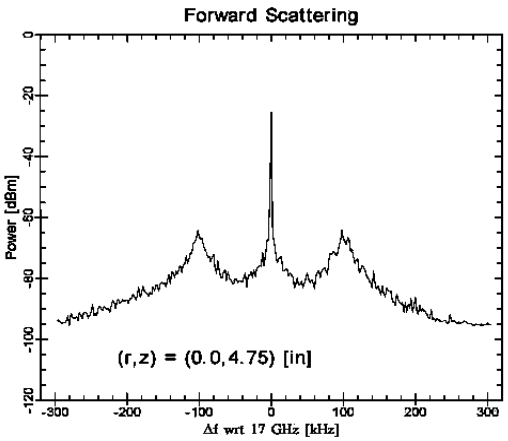

Figure 7a – Measured spectrum of the near field D-55 plasma plume.

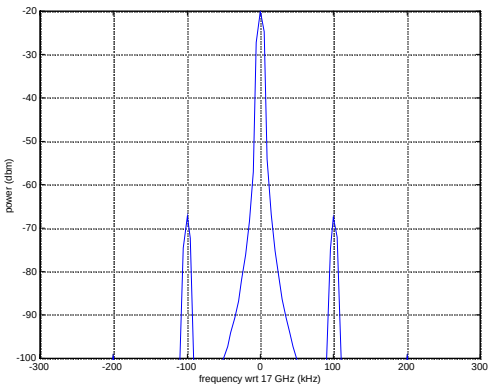

Figure 7b – Theoretical spectrum for the near field D-55 plasma plume

Based on these results, there is an indication that an azimuthal instability in a D-55 thruster tends to become more narrow and lower in amplitude downstream of the thruster's exit plane.

It was also possible to reproduce the sideband levels for the UM thruster as shown in Figure 9a and b. Setting the height of the instability to 0.3, the width to 10 cm, the distance from center to 3 cm, and the instabilities frequency of rotation to 12 kHz, we were able to obtain a spectrum with sidebands very close in amplitude to the measured spectrum. Unlike the D-55, the UM spectrum stays relatively constant down stream of the exit plane.

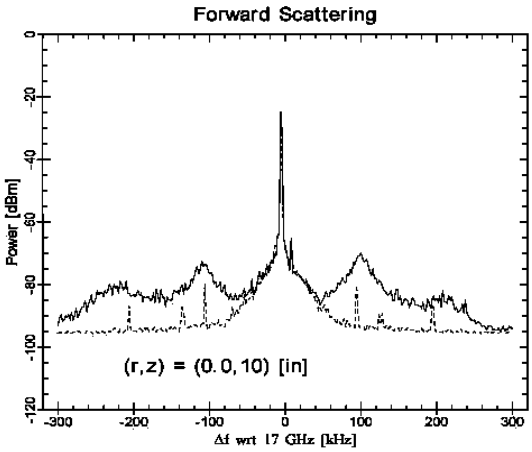

Figure 8a – Measured spectrum of the far field D-55 plasma plume.

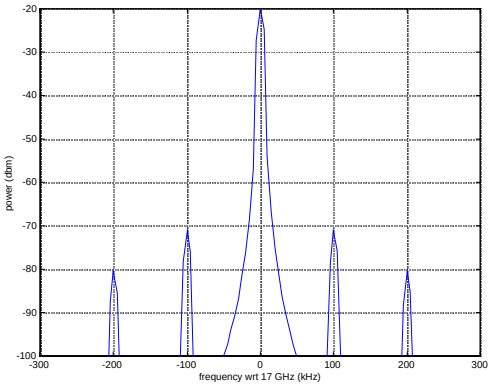

Figure 8b – Theoretical spectrum for the far field D-55 plasma plume.

Discussion and Summary

Based on the theoretical modeling of an azimuthal instability by the methods described, the following relationships between the instability model's parameters and calculated spectrum were found. As the width of the instability increases the relative amplitudes of the sidebands increases. As the height of the instability increases, the amplitude of all the sidebands increases, but the relative amplitudes of the sidebands remain constant. And, finally, as the distance the azimuthal instability is away from the center of the plume is varied different sidebands become more or less pronounced.

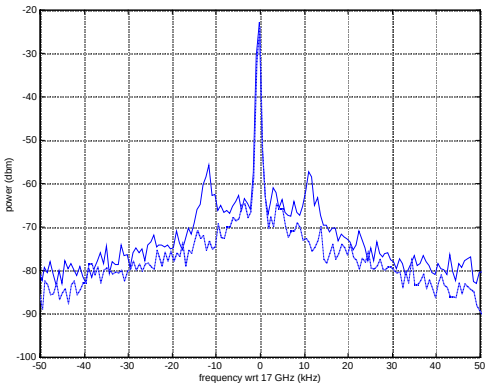

Figure 9a – Measured spectrum for the UM Thruster plasma plume.

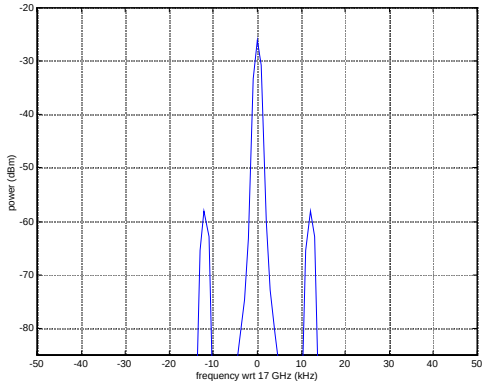

Figure 9b – Calculated spectrum for the UM Thruster plasma plume.

Some known limitations of azimuthal density model are the following. First, amplitude modulation due to beam spreading is not taken into account as it was in the axial model. Second, the antenna distribution needs to be taken into account instead of assuming a single plane wave. Thirdly, due to the symmetry of the electron density model used, spectral calculations done close to the middle of the plasma plume produce harmonics at double the instability rotational frequency. More work also needs to be done to see if such an azimuthal instability can be verified experimentally, such as with the use of in-situ probes.

In conclusion, we have noted that experimental measurements of frequency sidebands do not fully agree with simulations using existing models. We have proposed an alternative model that is based on known oscillation instabilities. The simulated results are more closely able to account for the observed variations.

Acknowledgments

This research was funded in part by AFOSR grant #F49620-95-1-0331 (contract monitor: Dr. M. Birkan). The authors would like to thank the students of the PEPL lab for their efforts to operate the thrusters and chamber systems.

Bibliography

1. Gilchrist, B. E., S. G. Ohler, A. D. Gallimore "Flexible Microwave System to Measure the Electron Number Density and Quantify the Communications Impact of Electric Thruster Plasma Plumes," *Rev. Sci. Inst.*, Vol. 68, No. 2, February, 1997.

2. Ohler, S.G., *Space Electric Propulsion Plasma Characterization Using Microwave and Ion Acoustic Wave Propagation*, Ph.D. Thesis, University of Michigan, 1996.

3. Ohler, S.G., *et al.*, RF Signal Impact Study of an SPT, paper AIAA 96-2706 presented at *32nd Joint Propulsion Conference*, Lake Buena Vista, FL, 1996.

4. Ohler, S.G., Gilchrist, B.E., and Gallimore, A.D., *Non-intrusive electron number density measurements in the plume of a 1 KW arcjet using a modern microwave interferometer.* IEEE Transactions on Plasma Science, **23**(3), p. 428-435, June, 1995.

5. Choueiri, E. Y., "Characterization of Oscillations in Closed Drift Thrusters," AIAA-94-3013, 30th Joint Propulsion Conference, Indianapolis, IN, June 27-29, 1994.

6. Hargus, W. A., N. Meezan, and M. A. Cappelli, "A study of a low power Hall thruster transient behavior," IEPC 97-058, 25th International Electric Propulsion Conference, Cleveland, OH, August 24-28, 1997.

7. Esipchuck, Y. B., A. Morozov, G. Tilinin, and A. Trofimov, "Plasma Oscillations in Closed Drift accelerators with an extended acceleration zone," Soviet Physics, Technical Physics, 18(7):928-932, 1974.

8. Esipchuck and G. Tilinin, "Plasma Oscillations in Closed Drift accelerators with an extended acceleration zone," Soviet Physics, Technical Physics, 21(4):417-423, 1976.

9. Dickens, J.C., Kristiansen, M., and O'Hair, E, *Plume Model of Hall Effect Plasma Thrusters with Temporal Consideration.* in IEPC 95-171. 1995, in *25rd International Electric, Propulsion Conference*, Moscow, Russia, 1995.

10. Gilchrist, B. G., C. N. Davis, A. D. Gallimore, "Electromagnetic Wave Scattering Experiments in Hall Thruster Plasma Plumes", paper presented at 35th Joint Propulsion Conference